

Self-Triggered Communication Enabled Control of Distributed Generation in Microgrids

Muhammad Tahir, *Member, IEEE*, and Sudip K. Mazumder, *Senior Member, IEEE*

Abstract—Efficient utilization of distributed generation (DG) resources in a microgrid requires coordinated control, which can be realized using multiagent-based system model. The coordinated control requires information exchange among the distributed agents, which can be implemented using either periodic or need-based aperiodic data transmission. For reducing the data communication requirements among the agents, an aperiodic self-triggered communication-based coordinated control is proposed. Centralized as well as distributed self-triggered coordinated control is implemented. The performance evaluation results show that self-triggered aperiodic communication requires lower data rates, while delivering the same performance as that of periodic sampled data control.

Index Terms—Communication network, distributed generation (DG), microgrid, self-triggered control.

I. INTRODUCTION

EFFECTIVE integration of multiple distributed generation (DG) units in microgrids plays an important role in the realization of smart-grid. For efficient utilization of each DG, a multilevel control is used. The primary control is responsible for maintaining the voltage and frequency stability, whereas the secondary control can be used to control the active and reactive power flow from the DG. Conventionally, the secondary control in a microgrid is based on a centralized control structure using periodic data transmissions, which requires higher communication rates and is prone to single point of failure. System reliability for secondary control in microgrids can be improved by using a distributed coordinated control approach.

For realizing the coordinated control of multiple DGs in microgrid, a multiagent-based system architecture can be employed [1]. In a multiagent system model of microgrid, each DG is considered as an agent. Multiagent-based systems have been used for load restoration [2] as well as power system secondary control [3]. Multiagent-based coordinated control has also successfully been used for power regulation in a multiple solar-cell-based distributed power generation system [4]. In addition, coordinated control using multiagent systems

has been proposed in [5] and has been applied to microgrids recently [6].

In coordinated multiagent control, the agents need to communicate with each other to exchange control and status information. Conventionally, for sampled data systems, the information is exchanged periodically among the agents. For a given sampling interval, the agent's state error is large at the next sampling instant, when there is a transient and correspondingly the sampling rate is chosen to meet the state error bound for the worst case transient. Using the same sampling rate for both transient and steady state results in large data transmission rates. On the other hand, due to network bandwidth constraint, an efficient use of underlying communication infrastructure is important from the system scaling perspective [7], [8]. In this context, employing need-based data exchanges among the agents, resulting in aperiodic information exchange has clear advantages compared to periodic data exchanges. The aperiodic data exchange can be realized using either event-triggered or self-triggered approach. Aperiodic event-triggered control of multiagent systems have been proposed recently [1], which provides the advantage of reduced communication while meeting the performance requirements.

Event-triggered data communication among multiple agents is reactive in nature and generates a response when the system state has deviated more than a certain threshold from a nominal value. On the other hand, self-triggered communication follows a proactive approach, which evaluates the next information exchange instance ahead of time. For event-triggered communication, continuous monitoring of the state variables is required, which results in a significant computational overhead. However, this is not the case for self-triggered communication, where agent states are only observed at the triggering instances [1]. Based on these facts, we have selected self-triggered mechanism for performing data communication among the agents in a multiagent-based microgrid for performing secondary control.

The continuous monitoring of the states in event-based control allows it to respond quickly in case of a larger disturbance. On the other hand, the self-triggered control can not respond immediately to disturbance. This is due to the fact that the next control update time instance is precomputed at the current time instant and state is not observed in between the two time instances.

This paper is organized as follows. In Section II, system architecture, detailing the communication network, and the control structure of the DG are outlined. The coordinated control of DGs in a microgrid, using multiagent-based self-triggered mechanism, is discussed in Section III. The performance evaluation results of the proposed approach

Manuscript received October 26, 2014; revised December 30 2014; accepted January 30, 2015. Date of publication February 11, 2015; date of current version March 27, 2015. Paper no. TII-14-1177.

M. Tahir is with the Department of Electrical Engineering, Al-Khwarizmi Institute of Computer Science, University of Engineering and Technology, Lahore 54890, Pakistan (e-mail: mtahir@uet.edu.pk).

S. K. Mazumder is with the Department of Electrical and Computer Engineering, University of Illinois at Chicago, Chicago, IL 60607, USA (e-mail: mazumder@ece.uic.edu).

Color versions of one or more of the figures in this paper are available online at <http://ieeexplore.ieee.org>.

Digital Object Identifier 10.1109/TII.2015.2402616

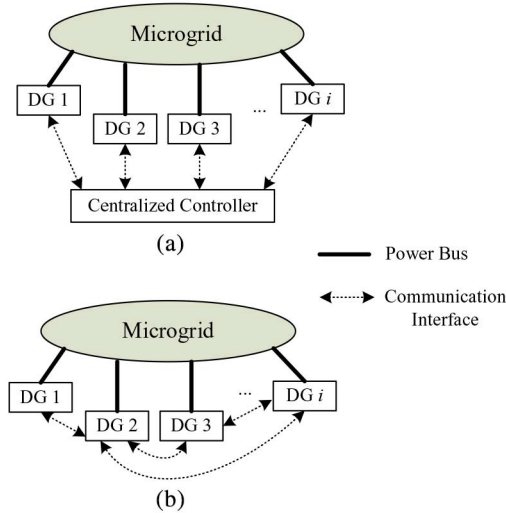


Fig. 1. (a) Centralized and (b) distributed control architecture and the corresponding information communication in a microgrid with multiple DG systems.

are provided in Section IV and we conclude our findings in Section V.

II. MICROGRID SYSTEM ARCHITECTURE

An arbitrary microgrid can have multiple DGs. The effective integration of DGs in a microgrid requires a hierarchical control involving primary (local) as well as secondary and tertiary (global) control of these resources [9]. The job of primary controller is to maintain the frequency and voltage stability, and can be achieved using fast local control [10], [11]. Response to any deviations to the voltage and frequency of the DGs is achieved by the secondary control, which is responsible for maintaining the references for the primary controller. In addition, the secondary control is also responsible for maintaining the active and reactive power flows from the DGs in a microgrid. It is worth mentioning that the microgrid can either operate in islanded mode or in grid connected mode. The frequency reference in islanded mode is generated locally, while in case of grid connected mode it is derived from the grid.

One possible solution to implement the secondary control is based on centralized structure, which requires each DG to communicate with a central controller, and can be realized using star communication structure. In star topology, a communication link exists between all DGs and the central controller as shown in Fig. 1(a). It is important to mention that one of the DGs can also serve the functionality of central controller. An alternative solution to this approach is based on a distributed control structure [10]. This distributed control requires only the neighboring DGs to communicate with each other to perform secondary control. The notion of neighbor is defined based on the existence of a link between the pair of DGs. The DG_j and DG_m are regarded as neighbors when they can communicate with each other. This scenario is illustrated in Fig. 1(b). A coordinated control of multiple DGs can be implemented either in centralized or distributed manner and requires to exchange active and reactive power parameters.

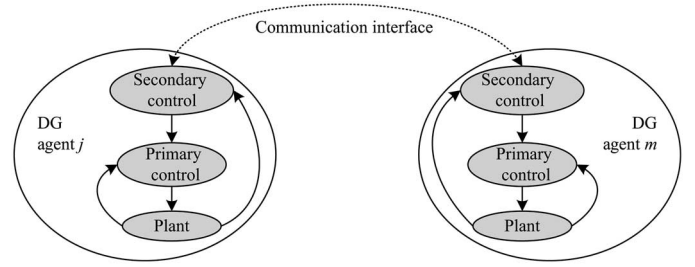


Fig. 2. Agent structure and communication interaction among the agents.

A. Communication Network Model

To implement the above-mentioned control architectures, we consider a collection of N DGs and define the corresponding set $\mathcal{N} = \{1, 2, \dots, N\}$. Each DG_j has an associated set of neighboring DGs denoted by $N_j \subset \mathcal{N}$. The set N_j includes all the DGs, which can communicate with DG_j and we assume that the underlying communication link is bidirectional. This scenario can be modeled using an undirected graph $G = \{N, E\}$, where E is the set of communication links among the communicating pairs of DGs.

For the graph G , we define an $N \times N$ adjacency matrix $A = A(G)$. Each entry $a_{j,m} \in A$ is set to 1 if we have $(j, m) \in E$, i.e., the corresponding communication link between DG_j and DG_m exists and to 0 otherwise. If $a_{j,m} = 1$, then we call DG_j and DG_m to be adjacent. From the communication perspective, the degree d_j of a DG_j is defined as the number of adjacent DGs to it and is given by $d_j = \sum_{m \in N_j, m \neq j} a_{j,m} \forall j$. Let $D \in R^{N \times N}$ is the diagonal matrix with entries $d_j, j \in \{1, 2, \dots, N\}$ and is called the degree matrix of graph G . Now, we can define the graph Laplacian matrix as $L = D - A$. The matrix L has all the row sums equal to zero, i.e., $L\mathbf{1} = 0$, where $\mathbf{1}$ is the vector of all ones. In the context of self-triggered communication, it is assumed that the information transmission delay among DGs is much smaller compared to the controller output update interval.

The agent structure to model DG and the communication interface for interactions among the agents is shown in Fig. 2. The structure of the agent has multilevel control, with local parameter sensing and actuation capability. In addition, the agent can switch between the islanded and grid connected modes of operation.

B. Control Structure of a DG

For the case of active and reactive power flow control from each DG, we can consider a *coordinated control problem*, where the neighboring DGs exchange their local power flow information to determine their share of power delivery to the grid. Specifically, let \tilde{P}_j and \tilde{Q}_j denote, respectively, the actual active and reactive powers delivered by the DG_j to the microgrid. To maintain the power balance in a microgrid, it is required that $\sum_j \tilde{P}_j = P_L$ and $\sum_j \tilde{Q}_j = Q_L$, where P_L and Q_L are the load active and reactive power requirements, respectively. It is important to realize that, specifically such a power balance in a microgrid is only possible in islanded mode of operation. In grid connected mode, the DGs in microgrid are

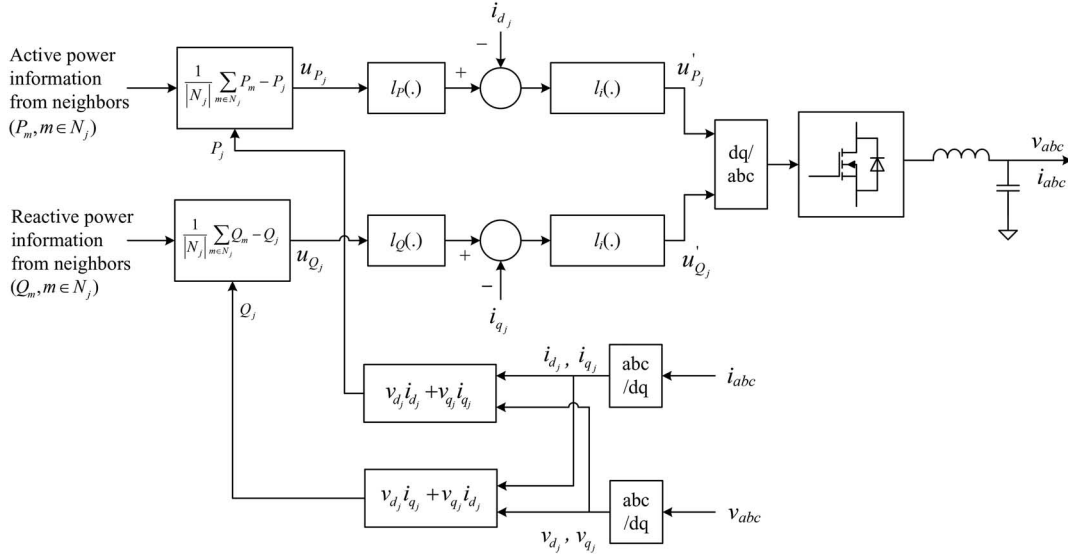


Fig. 3. Secondary control system architecture for the DG system in a microgrid.

usually responsible for partial power delivery and the remaining power is contributed by the utility. Let c_{P_j} and c_{Q_j} are the scaling coefficients to define scaled active power P_j and reactive power Q_j as

$$\begin{aligned} P_j &= c_{P_j} \tilde{P}_j \\ Q_j &= c_{Q_j} \tilde{Q}_j \quad \forall j. \end{aligned} \quad (1)$$

The scaling coefficients allow to have equal scaled power allocations to different DGs, while the actual power allocations being different. The use of scaling coefficients is extended in Section III-C, to account for uncertainties when renewable energy sources (RES) are used.

In a microgrid, the power from a DG is delivered to the grid using power electronic converters, which may be operating as voltage source inverters (VSI) or current source inverters (CSIs). The primary control in a DG is responsible for proper operation of these power-electronic converters. Fig. 3 illustrates one such inverter-based DG with current control implementation. The reference signals for the current control loop are generated by the DG's power flow assignment based on the consensus achieved by different DGs in a microgrid. In other words, each DG's secondary controller communicates with the neighboring DGs, and uses the received information to determine the reference parameters for primary controller. To achieve the power consensus among different DGs the power update control law, for DG_j is defined as

$$\Delta P_j(t_k^j) = \frac{1}{|N_j|} \sum_{m \in N_j} (P_m(t_k^m) - P_j(t_k^j)) \Delta t_k^j. \quad (2)$$

In (2), ΔP_j quantifies the difference in the power delivered by DG_j and the average power delivered by its neighbors at time instant t_k^j . Using different time instants for sampling power parameters at each DG will not mandate synchronization among the DGs and will allow distributed implementation. For centralized implementation, it is required that all the DGs have the same sampling instant, i.e., $t_k^m = t_k^j \forall m$, assuming DG_j is

responsible for implementing the centralized controller as well as synchronization among the DGs. A corresponding expression for reactive power update control law can be obtained along the same lines. The ΔP_j and correspondingly ΔQ_j are used to generate the reference signals as can be observed from the control structure block diagram shown in Fig. 3. Let L_j is the j th row vector of Laplacian matrix then the expression in (2) can be rewritten as

$$\frac{\Delta P_j}{\Delta t_k^j} = -\frac{1}{|N_j|} L_j P \quad (3)$$

where P is the vector of DG's powers defined as $P = [P_1 P_2 \cdots P_N]^T$ at their corresponding time instances. Ensuring Δt_k^j is small for $\forall k$, $\frac{\Delta P_j}{\Delta t_k^j}$ can be approximated by \dot{P}_j . We further simplify the notation by defining $\tilde{L}_j = \frac{1}{|N_j|} L_j$, which can be considered as the normalized Laplacian. Using the definition of \tilde{L}_j , now we can write the power update control for all the DGs as

$$\dot{P} = -\tilde{L}P. \quad (4)$$

The overall control signal, u'_{P_j} for DG_j, as can be observed from Fig. 3, is given by

$$u'_{P_j}(t) = l_i \left(l_P \left(\dot{P} \right) - i_{d_j} \right). \quad (5)$$

In (5), $l_P(\cdot)$ and $l_i(\cdot)$ are, respectively, linear compensators or controllers for active power and currents, whereas i_{d_j} is the active current supplied by DG_j. The active power control signal u_{P_j} is given by

$$u_{P_j}(t) = \dot{P}_j(t). \quad (6)$$

Combining (4) and (6), we have

$$u_P(t) = -\tilde{L}P(t). \quad (7)$$

The control law in (7) is responsible for ensuring that all the DGs meet the microgrid power requirements in a coordinated manner by exchanging necessary information among the neighboring DGs.

The convergence performance of power consensus among different DGs can be analyzed using spectral graph theory. In particular, the spectral properties of Laplacian matrix play an instrumental role in analyzing the convergence performance [12]. For an undirected graph, the matrix \tilde{L} is symmetric with the eigenvalues $\lambda_j, j \in \{1, 2, \dots, N\}$ all being real. The ordered sequence of eigenvalues is bounded as $0 = \lambda_1 \leq \lambda_2 \leq \dots \leq \lambda_N \leq 2$. When G is a connected graph, then the second smallest eigenvalue is strictly positive, i.e., $\lambda_2 > 0$. The rate of convergence of the consensus algorithm depends on the value of λ_2 [12], a larger value leads to faster convergence rate.

III. COORDINATED CONTROL OF DGs IN A MICROGRID

If one of the DGs is connected to all other DGs in a microgrid then it possible to implement centralized power control. If this is not the case, we can have a distributed implementation. These two possible power control solutions were discussed below. For implementing the coordinated power control discussed in the previous section, power information is exchanged either with the central controller or among the neighboring DGs depending on the type of controller used. Based on the advantages discussed above, self-triggered-based information exchange mechanism is used.

A. Centralized Control of DGs

In the centralized implementation, the power parameters are received from all the DGs at DG_j , which is responsible for implementing the power control. In self-triggered-based information communication, the controller at DG_j has to perform the following two tasks.

- 1) Update the power control output $u_{P_l} \forall l$ and convey this information to all DGs.
- 2) In addition, the controller determines the next time instant at which the next control action is to be performed.

The control output $\mathbf{u}_P(t)$ is updated at the discrete time instance corresponding to current update and is held constant, similar to the zero-order hold, till the next control update. This fact can be stated as $\mathbf{u}_P(t) = \mathbf{u}_P(t_k) \forall t \in [t_k, t_{k+1})$. Based on this fact, the expression in (8) can be rewritten as

$$\mathbf{u}_P(t) = \tilde{L}\mathbf{P}(t_k). \quad (8)$$

The actual power $\mathbf{P}(t)$ delivered by DGs continuously varies with time and correspondingly the error in power state variables, with respect to the last control action applied, can be defined as $\mathbf{e}(t) = \mathbf{P}(t_k) - \mathbf{P}(t)$ for $t \in [t_k, t_{k+1})$ and $\mathbf{e}(t) = [e_1 \ e_2 \ \dots \ e_N]^t$. To quantify the effectiveness of coordinated power control, a Lyapunov function $V(t) = \frac{1}{2}\mathbf{P}^T(t)\tilde{L}\mathbf{P}(t)$ is considered [13]. Then, we have

$$\dot{V}(t) = \mathbf{P}^T(t)\tilde{L}\dot{\mathbf{P}}(t). \quad (9)$$

Now using the fact that $\mathbf{u}_P(t) = \dot{\mathbf{P}}(t)$ and combining it with the expression in (8), we can rewrite (9) as

$$\dot{V}(t) = -\mathbf{P}^T(t)\tilde{L}\tilde{L}\mathbf{P}(t_k). \quad (10)$$

Substituting $\mathbf{P}(t_k) = \mathbf{P}(t) + \mathbf{e}(t)$, the expression in (10) becomes

$$\dot{V}(t) = -\|\tilde{L}\mathbf{P}\|^2 - \mathbf{P}^T(t)\tilde{L}\tilde{L}\mathbf{e}(t) \quad (11)$$

where $\|\cdot\|$ is the Euclidean norm. Introducing a scaling coefficient $\rho, \rho \in (0, 1)$, we define the error bound as

$$\|\tilde{L}\|\|\mathbf{e}(t)\| \leq \rho\|\tilde{L}\mathbf{P}\|. \quad (12)$$

For self-triggered information exchange among the nodes, the next time instant for information transmission and control update is precalculated at the current time. For $t \in [t_k, t_{k+1})$, we have by definition $\mathbf{P}(t) = -\tilde{L}\mathbf{P}(t_k)\Delta t_k + \mathbf{P}(t_k)$, where $\Delta t_k = t - t_k, t \in [t_k, t_{k+1})$. Using this fact, the error $\mathbf{e}(t)$ becomes $\tilde{L}\mathbf{P}(t_k)\Delta t_k$ and the expression in (12) can be rewritten as

$$\|\tilde{L}\mathbf{P}(t_k)\|\Delta t_k \leq \rho \frac{\|-\tilde{L}^2\mathbf{P}(t_k)\Delta t_k + \tilde{L}\mathbf{P}(t_k)\|}{\|\tilde{L}\|}. \quad (13)$$

An upper bound for t , which equals t_{k+1} , can be obtained by solving (13) for Δt_k and setting $\Delta t_k = t_{k+1} - t_k$. To obtain this upper bound, the inequality in (13) is converted to an equality and then can be written as

$$\|\tilde{L}\mathbf{P}(t_k)\|^2\|\tilde{L}\|^2(\Delta t_k)^2 = \rho^2\|\tilde{L}\mathbf{P}(t_k) - \tilde{L}^2\mathbf{P}(t_k)\Delta t_k\|^2. \quad (14)$$

Rearranging the terms in (14), after expanding the expression on right, we obtain

$$\left(\|\tilde{L}\mathbf{P}(t_k)\|^2\|\tilde{L}\|^2 - \rho^2\|\tilde{L}\mathbf{P}(t_k)\|^2\right)(\Delta t_k)^2 - \rho^2\|\tilde{L}^2\mathbf{P}(t_k)\|^2 + 2\rho^2(\tilde{L}\mathbf{P}(t_k))^T\tilde{L}\tilde{L}\mathbf{P}(t_k)(\Delta t_k) = 0. \quad (15)$$

Now solving (15) for Δt_k , we obtain

$$\Delta t_k = \frac{\gamma - \rho^2(\tilde{L}\mathbf{P}(t_k))^T\tilde{L}\tilde{L}\mathbf{P}(t_k)}{\|\tilde{L}\mathbf{P}(t_k)\|^2\|\tilde{L}\|^2 - \rho^2\|\tilde{L}\mathbf{P}(t_k)\|^2} \quad (16)$$

where γ is defined as

$$\gamma = \left\{ \rho^2\|(\tilde{L}\mathbf{P}(t_k))^T\tilde{L}\tilde{L}\mathbf{P}(t_k)\|^2 - (\|\tilde{L}^2\mathbf{P}(t_k)\|^2) \left(\|\tilde{L}\mathbf{P}(t_k)\|^2\|\tilde{L}\|^2 - \rho^2\|\tilde{L}\mathbf{P}(t_k)\|^2 \right) \right\}^{\frac{1}{2}}. \quad (17)$$

B. Distributed Control of DGs

In case of distributed implementation, only neighboring DGs communicate with each other and update their respective active and reactive powers. Let $t_0^j, t_1^j, \dots, t_k^j, \dots$, denote the control

update time instances for DG_j . The power measurement error for DG_j is defined by

$$e_j(t) = P_j(t_k^j) - P_j(t) \quad (18)$$

where $t \in [t_k^j, t_{k+1}^j)$. The DG_j control update using distributed implementation can be defined as

$$u_{P_j}(t) = \sum_{m \in N_j} P_m(t_{k_m}^m(t)) - P_j(t_k^j). \quad (19)$$

In (19), $t_{k_m}^m(t) = \min_{\{r \in \mathbb{N}; t_r^m \leq t\}} (t - t_r^m)$ where \mathbb{N} represents the set of natural numbers. In other words, $t_{k_m}^m(t)$ is the latest update time for DG_m . The control signal $u_{P_j}(t)$ is recomputed not only on its own update times t_0^j, t_1^j, \dots , but also at the update times of its neighbors $t_0^m, t_1^m, \dots \forall m \in N_j$. Using the definition of $t_{k_m}^m(t)$, it can be implied that

$$P_m(t_{k_m}^m(t)) = P_m(t) + e_m(t). \quad (20)$$

Define $y_j(t) = \tilde{L}_j \mathbf{P}(t)$, which can be rewritten as

$$y_j(t) = P_j(t) - \frac{1}{|N_j|} \sum_{m \in N_j} P_m(t). \quad (21)$$

Combining $y_j(t)$ from above expression with (9), we obtain

$$\begin{aligned} \dot{V}(t) &= - \sum_j y_j^2(t) - \sum_j \sum_{m \in N_j} y_j(t)(e_j(t) - e_m(t)) \\ &= - \sum_j (y_j^2(t) + |N_j| y_j(t) e_j(t)) \\ &\quad + \sum_j \sum_{m \in N_j} y_j(t) e_m(t). \end{aligned} \quad (22)$$

Now using the inequality $2|x_1 x_2| \leq c x_1^2 + \frac{1}{c} x_2^2$, $c > 0$ with (22), we obtain

$$\begin{aligned} \dot{V}(t) &\leq - \sum_j (y_j^2(t) - c|N_j| y_j^2(t)) + \sum_j \frac{|N_j|}{2c} e_j^2(t) \\ &\quad + \sum_j \sum_{m \in N_j} \frac{1}{2c} e_m^2(t). \end{aligned} \quad (23)$$

Due to the symmetry of \tilde{L} , the last term on right-hand side in (23) can be simplified as $\sum_j \sum_{m \in N_j} \frac{1}{2c} e_m^2(t) = \sum_j \frac{|N_j|}{2c} e_j^2(t)$. It should be noted that the expression in (23) is upper bounded by 0. Now ensuring $0 < c < \frac{1}{|N_j|} \forall j \in N$ and introducing a scaling constant ρ_j $0 \leq \rho_j \leq 1$, the expression in (23) can be rewritten as

$$e_j^2(t) \leq \rho_j \frac{c(1 - c|N_j|)}{|N_j|} y_j^2(t). \quad (24)$$

Starting with expression $\dot{P}_j(t) = \frac{1}{|N_j|} \sum_{m \in N_j} (P_m(t_{k_m}^m(t)) - P_j(t_k^j))$, it can be expanded to

$$P_j(t) = - \frac{1}{|N_j|} \sum_{m \in N_j} (P_j(t_k^j) - P_m(t_{k_m}^m(t))) (\Delta t_k^j) + P_j(t_k^j). \quad (25)$$

In (25), $\Delta t_k^j = t - t_k^j$ for $t \in [t_k^j, t_{k+1}^j)$. Defining $\delta_j = \frac{1}{|N_j|} \sum_{m \in N_j} (P_j(t_k^j) - P_m(t_{k_m}^m(t)))$ and substituting (25) in (21), we obtain

$$\begin{aligned} y_j(t) &= - \frac{1}{|N_j|} \sum_{m \in N_j} (-\delta_m(t - t_{k_m}^m(t)) + P_j(t_{k_m}^m(t))) \\ &\quad + \delta_j \Delta t_k^j - P_j(t_k^j) \\ &= -\delta_j \Delta t_k^j + \frac{1}{|N_j|} \sum_{m \in N_j} (P_j(t_k^j) - P_j(t_{k_m}^m(t))) \\ &\quad + \frac{1}{|N_j|} \sum_{m \in N_j} \delta_m(t - t_k^j + t_k^j - t_{k_m}^m(t)) \end{aligned} \quad (26)$$

which is simplified to

$$\begin{aligned} y_j(t) &= \left(\frac{1}{|N_j|} \sum_{m \in N_j} \delta_m - \delta_j \right) \Delta t_k^j \\ &\quad + \delta_j + \frac{1}{|N_j|} \sum_{m \in N_j} \delta_m (t_k^j - t_{k_m}^m(t)). \end{aligned} \quad (27)$$

By denoting $\Omega_j = \delta_j + \frac{1}{|N_j|} \sum_{m \in N_j} \delta_m (t_k^j - t_{k_m}^m(t))$ and $\delta'_j = \frac{1}{|N_j|} \sum_{m \in N_j} \delta_m - \delta_j$ in the expression in (27) and substituting it in (24), we obtain

$$e_j^2(t) \leq \rho_j \frac{c(1 - c|N_j|)}{|N_j|} (\delta'_j \Delta t_k^j + \Omega_j)^2. \quad (28)$$

Denoting $\eta_j = \frac{c(1 - c|N_j|)}{|N_j|}$ and using $e_j(t) = P_j(t) - P_j(t_k^j)$, (28) becomes

$$(P_j(t) - P_j(t_k^j))^2 \leq \rho_j \eta_j (\delta'_j \Delta t_k^j + \Omega_j)^2. \quad (29)$$

Using (25) and definition of δ_j , we can rewrite (28) as

$$(\delta_j (\Delta t_k^j))^2 \leq \rho_j \eta_j (\delta'_j \Delta t_k^j + \Omega_j)^2 \quad (30)$$

which after rearranging the terms can be written as

$$(\delta_j^2 - \rho_j \eta_j \delta_j'^2) (\Delta t_k^j)^2 - 2\rho_j \eta_j \Omega_j \delta_j' (\Delta t_k^j) \leq \rho_j \eta_j \Omega_j^2. \quad (31)$$

The upper bound for Δt_k^j is obtained by solving (31) for equality and results in

$$\Delta t_k^j = \frac{(\rho_j \eta_j)^{\frac{1}{2}} \Omega_j ((\rho_j \eta_j)^{\frac{1}{2}} \delta_j' \pm \delta_j)}{\delta_j^2 - \rho_j \eta_j \delta_j'^2}. \quad (32)$$

For obtaining next update instance, Δt_k^j is chosen as the positive solution to (32), which can be obtained as

$$\Delta t_k^j = \max \left\{ 0, \frac{(\rho_j \eta_j)^{\frac{1}{2}} \Omega_j}{\delta_j - (\rho_j \eta_j)^{\frac{1}{2}} \delta_j'}, \frac{-(\rho_j \eta_j)^{\frac{1}{2}} \Omega_j}{\delta_j + (\rho_j \eta_j)^{\frac{1}{2}} \delta_j'} \right\}. \quad (33)$$

Using similar procedure, the update time instances for the reactive power control can be obtained as well.

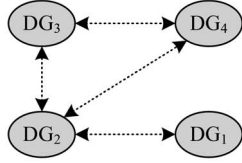


Fig. 4. System configuration of four DGs along with communication structure.

C. Model Extension

It is quite possible that the DGs in a microgrid are fed from RES. In that case, the uncertainty due to RES can be incorporated in the proposed self-triggered coordinated control by using a switching network model. A switching network can be modeled using a dynamic graph [12], which can model the node or link failures as well as outages due to RES intermittency. Specifically, when the DG in a microgrid is fed from an RES, then it is quite possible that it can no longer deliver the power and has to be disconnected from the system. The scenario can be modeled using a dynamic graph, which results in topology switching of the network. For that purpose, dynamic graph $G_{s(t)}$ parametrized by the switching signal $s(t) : R \rightarrow S$, which takes values in the index set $S = \{1, 2, \dots, s\}$ is defined. Using the dynamic graph, the expression in (4) can be rewritten as

$$\dot{P} = -\tilde{L}(G_\alpha)P \quad (34)$$

where the topology index $\alpha = s(t) \in S$. The convergence rate for this dynamic graph is controlled by $\lambda_2^* = \min_{\alpha \in S} \lambda_2(G_\alpha)$ [12]. Since for the connected graph $\lambda_2^* > 0$, the agent's state converge at a rate equal to or faster than λ_2^* , for any arbitrary switching signal.

The scaling coefficients in (1) can be redefined as an element of an indexed set, i.e., $c_{P_j} \in \{c_P^{(1)}, c_P^{(2)}, \dots, c_P^{(\mu)}\}$ and $c_{Q_j} \in \{c_Q^{(1)}, c_Q^{(2)}, \dots, c_Q^{(\nu)}\}$. The choice of specific c_P^β and c_Q^γ , where $\beta \in \{1, 2, \dots, \mu\}$, $\gamma \in \{1, 2, \dots, \nu\}$ is based on the current operating point of the DG, which can in turn depend simultaneously on the following.

- 1) The current power deliverance point of the RES.
- 2) Any adjustment required by the load active and reactive power demand, which is achieved by selecting appropriate values of \tilde{P}_j and \tilde{Q}_j on the PQ -curve of the RES [14]. The choice of \tilde{P}_j, \tilde{Q}_j pair on the PQ -curve of an RES also allows to tradeoff between active and reactive powers delivered by the respective RES.

D. Performance Evaluation Results

The coordinated power flow control by these DGs can be realized using either centralized or distributed implementation. For simulation results, we have considered a network of four DGs. Fig. 4 illustrates the connectivity among the DGs. For information exchange, it is assumed that each DG is equipped with IEEE 802.15.4-based communication interface. For the centralized implementation, DG₂ assumes the role of central

TABLE I
SYSTEM PARAMETERS USED FOR SIMULATIONS

Parameter name	Value
DG1 and DG2 rating	30, 15 kVA
DG3 and DG4 rating	37, 45 kVA
Proportional and integral gains for l_P and l_Q	0.4, 0.02
Proportional and integral gains for l_i	0.5, 0.03
System load	70 kW
Communication rate among DGs	250 Kbps

node. The normalized Laplacian matrix used for the simulation setup is given by

$$\tilde{L} = \begin{bmatrix} 1 & -1 & 0 & 0 \\ -1/3 & 1 & -1/3 & -1/3 \\ 0 & -1/2 & 1 & -1/2 \\ 0 & -1/2 & -1/2 & 1 \end{bmatrix}. \quad (35)$$

In our implementation, each DG comprises a controller module, an energy source and a power converter. The controller module consists of first-order linear secondary controllers $l_P(\cdot)$, $l_Q(\cdot)$ and primary current controller $l_i(\cdot)$. The proposed coordinated power control algorithm is implemented for the microgrid islanded mode of operation. The inductor and capacitor of the output filter, the $l_P(\cdot)$, $l_Q(\cdot)$, and $l_i(\cdot)$ controllers as well as the control law $u_{P_j} = \dot{P}_j$, all contribute to the dynamic states of the DG. The system parameters used to obtain simulation results are tabulated in Table I.

The information communication requirement, in terms of packet transmission rate, for self-triggered implementation is compared with that of periodic sampled data system. In addition, the packet rate requirement for centralized self-triggered implementation is also compared against the distributed self-triggered implementation. For fair comparison between centralized and distributed self-triggered implementations, we require $\rho_j = \rho \forall j$. The number of packets to be exchanged per iteration for centralized implementation is proportional to the number of DGs in the system, i.e., $|\mathcal{N}|$. On the other hand, for distributed implementation, the number of packets exchanged by DG _{j} depends on the number of its neighbor DGs, i.e., $|N_j|$ and the total number of packets for distributed implementation are proportional to $\sum_j |N_j|$.

The packet rate requirements for periodic as well as self-triggered data transmission are compared in Fig. 5. The sampled data packet transmission rate is chosen to meet the worst case state error requirement corresponding to a transient (as discussed previously in Section I) and as a result requires higher packet rate as can be observed from Fig. 5. In addition, from Fig. 5, it can be observed that distributed implementation requires a higher packet rate compared to the centralized case. This can be attributed to the fact that the lower bound for $\sum_j |N_j|$ is given by $|\mathcal{N}|$, i.e., each DG has only one neighbor, which is the minimum requirement to ensure the connectivity among the DGs. The difference between $\sum_j |N_j|$ and $|\mathcal{N}|$ depends on the average number of neighboring DGs in a microgrid and is mainly responsible for the packet rate requirement

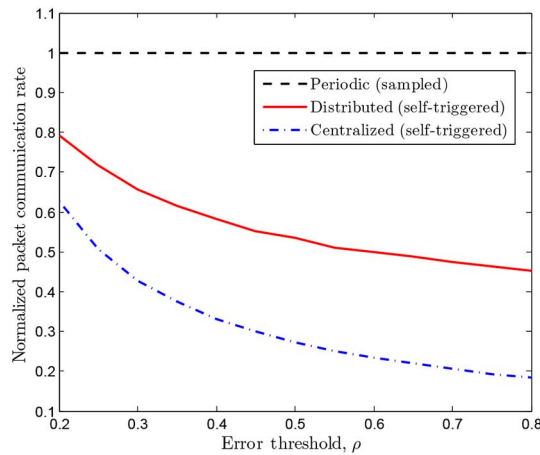


Fig. 5. Packet rate requirement comparison of for centralized and distributed self-triggered communication with that of sampled data system.

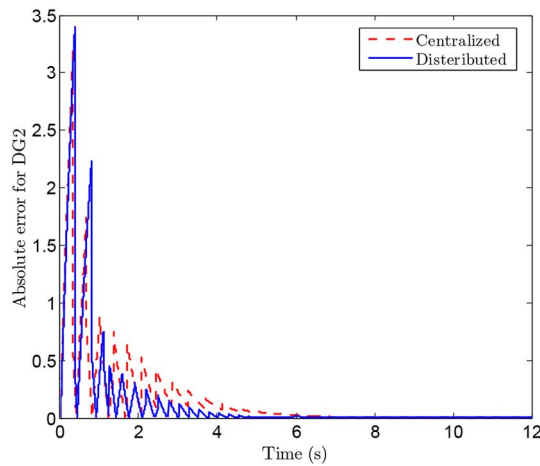


Fig. 6. Absolute power error for DG2 based on (18) for two implementations of self-triggered mechanism.

gap for distributed and centralized implementations of self-triggered communication mechanism.

From (18), the power error magnitude $|P_j(t_k^j) - P_j(t)|$ is responsible for deciding the next triggering time instant for information exchange among the DGs. In case of distributed implementation, the next triggering instant for DG_j not only depends on its own power error magnitude but also on its neighboring DGs error magnitude. On the other hand, for centralized case, the triggering instant is based on error norm of all the DGs. A comparison of power error magnitude for distributed and centralized implementations is shown in Fig. 6. It can be observed from Fig. 6 that the number of triggering events is larger for distributed case resulting in higher packet rate requirement.

The power sharing among different DGs, using distributed self-triggered communication mechanism, is shown in Fig. 7. The time update instances based on self-triggered mechanism correspond to the power jump instances as can be observed from Fig. 7. At each time instance, the overshoot in the

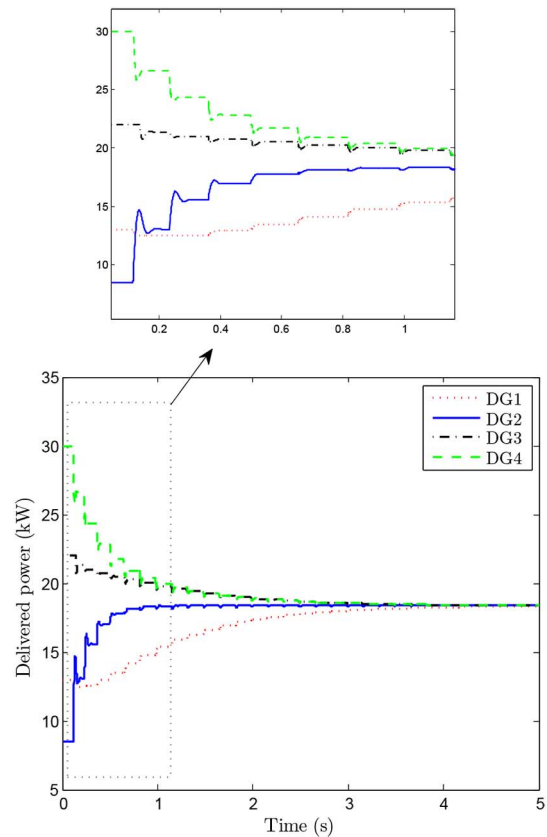


Fig. 7. Power distribution among the DGs using distributed self-triggered communication for equal power sharing.

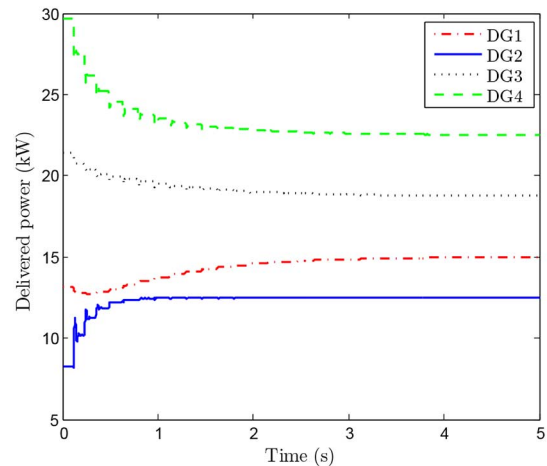


Fig. 8. Power distribution among the DGs using distributed self-triggered communication with proportional power sharing.

power adjustment is dependent on the gain parameters used by the linear controllers. The power control result for unequal power distribution among different DGs is shown in Fig. 8. In this case, the power delivered by each DG is required to be proportional to its kVA rating.

Finally, the convergence performance in case of load transient with unequal load sharing is evaluated for centralized

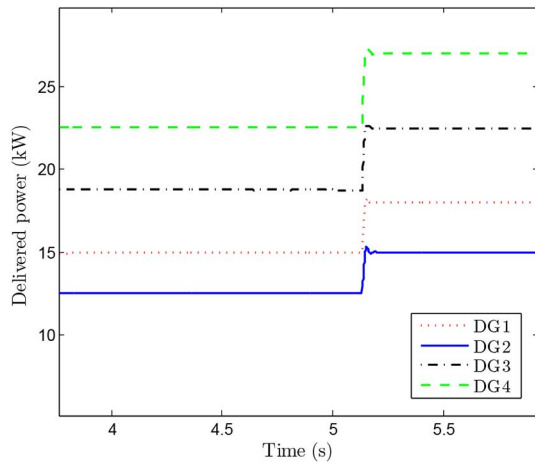


Fig. 9. Load transient and the resulting load distribution among different DGs for the centralized self-triggered implementation. DG₂ is assigned the central node functionality.

self-triggered implementation. For that purpose, the system load is increased by 20% and the corresponding load increase for each DG can be observed from the result in Fig. 9. Before the load transient, all the DGs were delivering power proportionally to their capacity. When the load transient happens, the resulting increase in the load is also shared proportionately by each DG as can be seen from Fig. 9.

The distributed implementation of self-triggered mechanism has the advantage of withstanding the single point of failure. For instance, if the communication link of the node implementing the centralized controller fails, then no coordination among the DGs will be possible. One possible solution to this problem is to have some other DG(s) equipped with centralized controller capability. In contrast, the failure of the communication link of an arbitrary DG in case of distributed implementation allows the remaining DGs to continue functioning by coordinating. However, the centralized implementation has the advantage of reduced communication or packet rate requirement as verified by the results.

IV. CONCLUSION

Multiagent-based coordinated control can be used for efficient integration of DG resources in microgrid. Self-triggered aperiodic communication employed for coordinated control leads to reduced data transmission rates among the agents. Both distributed and centralized realizations for self-triggered aperiodic control have been evaluated and compared against periodic sampled data-based counterpart. A reduction in the data rate requirement is observed for self-triggered-based consensus control.

For distributed self-triggered implementation, point to point communication is performed among the neighboring DGs. However, in centralized implementation the central DG makes a control output broadcast to every other DG and is the main reason for reduced communication rate. Using higher data

rates for information exchange among the DGs can provide an improved convergence performance for coordinated power control.

REFERENCES

- [1] D. V. Dimarogonas, E. Frazzoli, and K. H. Johansson, "Distributed event-triggered control for multi-agent systems," *IEEE Trans. Autom. Control*, vol. 57, no. 5, pp. 1291–1297, May 2012.
- [2] Y. Xu and W. Liu, "Novel multiagent based load restoration algorithm for microgrids," *IEEE Trans. Smart Grid*, vol. 2, no. 1, pp. 152–161, Mar. 2011.
- [3] A. Bidram, A. Davoudi, and F. Lewis, "A multi-objective distributed control framework for islanded ac microgrids," *IEEE Trans. Ind. Informat.*, vol. 10, no. 3, pp. 1785–1798, Aug. 2014.
- [4] H. Xin, Z. Qu, J. Seuss, and A. Maknouninejad, "A self-organizing strategy for power flow control of photovoltaic generators in a distribution network," *IEEE Trans. Power Syst.*, vol. 26, no. 3, pp. 1462–1473, Aug. 2011.
- [5] W. Yu, L. Zhou, X. Yu, J. Lu, and R. Lu, "Consensus in multi-agent systems with second-order dynamics and sampled data," *IEEE Trans. Ind. Informat.*, vol. 9, no. 4, pp. 2137–2146, Nov. 2013.
- [6] Y. Cao, W. Yu, W. Ren, and G. Chen, "An overview of recent progress in the study of distributed multi-agent coordination," *IEEE Trans. Ind. Informat.*, vol. 9, no. 1, pp. 427–438, Feb. 2013.
- [7] Q. Yang, J. A. Barria, and T. C. Green, "Communication infrastructures for distributed control of power distribution networks," *IEEE Trans. Ind. Informat.*, vol. 7, no. 2, pp. 316–327, May 2011.
- [8] S. K. Mazumder, K. Acharya, and M. Tahir, "Joint optimization of control performance and network resource utilization in homogeneous power networks," *IEEE Trans. Ind. Electron.*, vol. 56, no. 5, pp. 1736–1745, May 2009.
- [9] J. M. Guerrero, J. C. Vasquez, J. Matas, L. G. de Vicuña, and M. Castilla, "Hierarchical control of droop-controlled AC and DC microgrids—A general approach toward standardization," *IEEE Trans. Ind. Electron.*, vol. 58, no. 1, pp. 158–172, Jan. 2011.
- [10] A. Bidram, A. Davoudi, F. L. Lewis, and Z. Qu, "Secondary control of microgrids based on distributed cooperative control of multi-agent systems," *IET Gener. Transm. Distrib.*, vol. 7, no. 8, pp. 822–831, Aug. 2013.
- [11] S. K. Mazumder, M. Tahir, and K. Acharya, "Master-slave current-sharing control of a parallel DC-DC converter system over an RF communication interface," *IEEE Trans. Ind. Electron.*, vol. 55, no. 1, pp. 59–66, Jan. 2008.
- [12] R. Olfati-Saber, J. A. Fax, and R. M. Murray, "Consensus and cooperation in networked multi-agent systems," *Proc. IEEE*, vol. 95, no. 1, pp. 215–233, Jan. 2007.
- [13] H. K. Khalil and J. Grizzle, *Nonlinear Systems*. Upper Saddle River, NJ, USA: Prentice-Hall, 2002.
- [14] N. R. Ullah, K. Bhattacharya, and T. Thiringer, "Wind farms as reactive power ancillary service providers, technical and economic issues," *IEEE Trans. Energy Convers.*, vol. 24, no. 3, pp. 661–672, Sep. 2009.



Muhammad Tahir (M'02) received the Ph.D. degree in electrical and computer engineering from the University of Illinois at Chicago, Chicago, IL, USA, in 2008.

He is an Associate Professor with the Department of Electrical Engineering, University of Engineering and Technology Lahore, Lahore, Pakistan. He was a Visiting Research Scholar at the University of Illinois at Chicago, in 2014. He has been the Principal Investigator on the funded research projects related to air quality monitoring and intelligent camera networks. He has authored more than 40 international publications to his credit. He is the Reviewer of numerous IEEE journals and conferences. His research interests include wireless sensor networks, delay tolerant networks, distributed resource optimization for wireless networks, and real-time wireless multimedia networks.



Sudip K. Mazumder (S'97–M'01–SM'03) received the Ph.D. degree in electrical and computer engineering from Virginia Tech, Blacksburg, VA, USA, in 2001.

He is a Professor with the Department of Electrical and Computer Engineering, University of Illinois (UIC), Chicago, IL, USA. He has over 23 years of professional experience, and has held R&D and design positions in leading industrial organizations, and served as a Consultant for several industries.

Since 2008, he has served as the President of NextWatt LLC, Hoffman Estates, IL. Since joining UIC, he has been awarded about 40 sponsored projects by National Science Foundation (NSF), Department of Energy (DOE), Office of Naval Research (ONR), Advanced Research Project Agency - Energy (ARPA-E), California Energy Commission (CEC), Environmental Project Agency (EPA), Air Force Research Laboratory (AFRL), National Aeronautics and Space Administration (NASA), Naval Sea Systems Command (NAVSEA), and multiple leading industries. He has authored over 180 journal and conference papers and 9 book/book chapters, presented 65 invited presentations, and holds 8 issued and several pending patents.

Dr. Mazumder served/serves as the Guest Editor-in-Chief and Associate Editor for multiple IEEE Transactions, and was the first Editor-in-Chief for *Advances in Power Electronics*. He has served and is serving in high-profile capacities in leading IEEE conferences, technical committees, and NSF panels. He was the recipient of the several prestigious awards including UIC's Inventor of the Year Award (2014), University of Illinois' University Scholar Award (2013), IEEE Power Electronics Society (PELS) Transaction Prize Paper Award (2001), IEEE Future Energy Challenge Award (2005), ONR Young Investigator Award (2005), and NSF CAREER Award (2003).